

Influence of Zirconia Incorporation on the Mechanical and Chemical Properties of Ni-Co Alloys

Meenu Srivastava*, A Srinivasan, V K William Grips

Surface Engineering Division, Council of Scientific and Industrial Research, National Aerospace Laboratories, Bangalore, 560017, India

Abstract Ni-Co-ZrO₂ nano-composites are electrodeposited from sulphamate electrolyte and a comparison is made with Ni-ZrO₂ in terms of structure and properties. The Co content in the coatings is in the range of 10-80wt%. The deposition conditions like current density, pH are optimized in terms of microhardness and amounts of ZrO₂ incorporated. The microhardness studies revealed that the maximum hardness is exhibited by Ni-28Co-2ZrO₂ composite. The FESEM study showed a change in morphology from polyhedral to ridge with increase in Co content from 10 to 80wt%. A change in crystal structure from fcc to hcp is also seen. The effect of annealing treatment in terms of microhardness is studied by subjecting the composite electroforms to 800°C. The Co rich composite exhibited better stability compared to Ni rich composites. Ni-28Co-2ZrO₂ composite exhibited better immersion corrosion resistance while, Ni-ZrO₂ composite displayed better electrochemical corrosion resistance. The wear studies showed that Ni-10Co-2ZrO₂, Ni-28Co-2ZrO₂ composites showed better resistance. Thus, it is seen that the coatings can be tailored to suit various applications.

Keywords Metal matrix composites, Ni-Co-ZrO₂, Tribology, Wear, Corrosion, Electrochemical Study

1. Introduction

Corrosion and wear destroy national wealth in multibillion dollar range annually. Modern high performance components are subjected to extreme temperatures and mechanical stress, and thus require surface protection against high temperature and mechanical wear and tear. A highly versatile and low cost technique must be selected to apply protective coatings, one such technique is electroplating.¹ Composite electroplating involves the co-deposition of insoluble metallic or non-metallic compounds in a metal or alloy matrix. Such composite coating features the properties of both the matrix and the dispersed phase. The coatings are called as metal matrix composites (MMC) when the matrix involved is a metal. Composite coatings comprising of various dispersed phases like SiC, Si₃N₄, Al₂O₃, CeO₂, TiO₂, YSZ etc have been developed for diverse applications.²⁻¹⁰ The composite system considered in the present study comprises of Ni-Co alloy as the matrix. The benefit of choosing Ni-Co alloy as matrix lies in the fact that alloying of Ni with Co strengthens it by forming a solid solution which helps to improve wear, corrosion resistance and also improves the high temperature properties.^{11,12} The dispersed phase chosen is zirconia ZrO₂, as it is known to possess excellent properties such as

mechanical strength, chemical inertness, thermal stability, wear and corrosion resistance.¹³ Its good thermal matching with metals makes it suitable for protective coatings.^{14,15} It is also a promising constituent present in the transition metal based catalysts used in exhaust gas purifying devices.¹⁶ Depending on its crystalline structure it can be an insulator used as high resistance ceramic or an n-type semiconductor.¹⁵ ZrO₂ exists as a polymorph, namely cubic, tetragonal and monoclinic.¹⁷ The effect of incorporation of ZrO₂ in Ni matrix has been extensively reported.^{13,18-24} Reddy et al have reinforced tetragonal ZrO₂ in Ni matrix by pulsed electrodeposition. A 16% increase in microhardness of the composite has been reported.²³ The composite on annealing (50-200°C) showed an increase in the microhardness followed by a substantial decrease upto 300°C. Effect of heat treatment on the incorporation of ZrO₂ in Ni-Co matrix has not been studied much.²⁵ Zhang et al have reported brush plating of Ni-Co-ZrO₂ composite coating to repair the wear surface of the die casting dies of H13. The coating improved the surface hardness, wear resistance and oxygen resistance of dies.

The present study is aimed at incorporating ZrO₂ nano-particles in Ni-Co alloy matrices by electrodeposition method, and studying its influence on the thermal, mechanical and chemical properties.

2. Experimental

The Ni/Ni-Co-ZrO₂ nano-composites were electroformed from a conventional additive free sulphamate electrolyte of

* Corresponding author:

meenusr@nal.res.in (Meenu Srivastava)

Published online at <http://journal.sapub.org/materials>

Copyright © 2011 Scientific & Academic Publishing. All Rights Reserved

composition Nickel sulphamate 275g L^{-1} , nickel chloride 6gL^{-1} , boric acid 30gL^{-1} and SLS 0.2gL^{-1} . Co was added as cobalt sulphamate and the additions were made so as to obtain Co content in the range of 10-80wt%. ZrO_2 particles of size 20-30nm and monoclinic crystal structure were procured from M/s Nanostructured and Amorphous Materials, USA were used in this study. Particle content of 25gL^{-1} was dispersed in the electrolyte by magnetic stirring for a period of 16hrs prior to electrodeposition. The Ni-Co- ZrO_2 composites were deposited galvanostatically under ambient conditions using optimized conditions of pH 4.0 and current density 0.8Adm^{-2} . The coating was deposited on a mild steel substrate (cathode) of plating dimension $0.05\text{m} \times 0.0375\text{m}$ using Ni sheet as anode of size $0.05\text{m} \times 0.05\text{m}$. During the process of electrodeposition, the ZrO_2 nano-particles were kept under suspension by magnetic stirring at a speed of 400rpm. The composite coatings were prepared metallographically and subjected to microhardness testing. The hardness was tested using the Knoop's indenter (Buehler Microhardness tester Micromet 100) employing a load of 0.050kgf. The readings reported are the average of various measurements performed at different locations. The uniformity of ZrO_2 distribution was analyzed using optical microscopy. The surface morphology of the coatings was studied using Field Emission Scanning Electron Microscope (FESEM), Carl Zeiss Supra 40 VP and ZrO_2 , Co content in the coatings was determined using Energy Dispersive X-ray analysis (EDX). The crystal structure and the phases were identified using X-ray diffraction (XRD) studies. The crystallite size of the coatings was determined using Scherrer formula $D = K\lambda(\beta\cos\theta)^{-1}$ where, K is the Scherrer factor ≈ 1 , D the crystallite size, λ the incident radiation wavelength, β is the integral breadth of the structurally broadened profile and θ is the angular position.²⁶ The thermal stability of the coatings was studied by subjecting the composite electroforms to isothermal annealing at temperatures ranging from 200°C - 800°C in intervals of 200°C for a duration of 1 hour. The thermal stability has been expressed in terms of microhardness. The corrosion resistance of the coatings was determined by immersion method and also by electrochemical polarization technique. The immersion test has been performed by immersing the composite electroforms in 3.5% NaCl medium for 168hrs and the corrosion rate is expressed in terms of weight loss. A comparison was made with polarization and electrochemical impedance studies. These studies were carried out in a conventional three-electrode corrosion cell using a CHI604 2D (CH Instruments) test system. In the tests, specimen of area 1cm^2 was exposed to the electrolyte (3.5% NaCl). The saturated calomel electrode was used as a reference, and platinum served as a counter electrode. The tests were performed under room temperature conditions. Prior to the experiment the samples were immersed in the electrolyte for 45mins to attain the open circuit potential (OCP) or steady state potential. After the stabilization of OCP the upper and lower potential limits were fixed to $\pm 200\text{mV}$ with respect to the OCP for carrying out the polarization studies. The Impedance measurements were

performed in the frequency range of 10m Hz to 100 kHz and an amplitude of 10mV was applied on the OCP. All the measured data are presented as Nyquist and Bode plots. The wear resistance of the coatings has been analyzed under dry sliding conditions using Pin-on-disc wear tester (DUCOM India) and wear rate is expressed in terms of wear volume loss. The wear testing conditions are discussed in detail elsewhere.²⁷ The volumetric wear loss V was determined using the equation: $V = \pi h^2 (r - h/3)$ ¹⁷ where r is the radius of the hemispherical pin and h is the wear height loss of the pin.

3. Results and Discussion

3.1. Ni- ZrO_2 Co-deposition

The deposition conditions were optimized with reference to Ni- ZrO_2 composite coating in terms of microhardness. The pH was varied in the range of 2.5 to 4.5 and the current density in the range of 0.8 to 6.4Adm^{-2} . The variation in microhardness and the extent of ZrO_2 incorporation (Vol %) in the coating with respect to pH are shown in Figure 1.

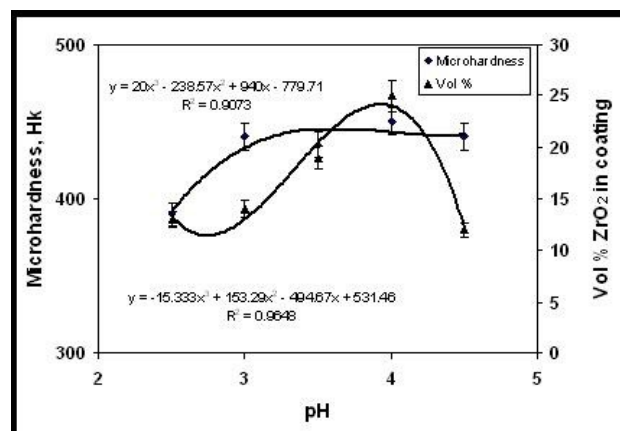


Figure 1. Correlation between pH and Microhardness, Vol % of ZrO_2 incorporated in the coating

It is seen from the figure that the equation that fits best between pH, microhardness and Vol% of ZrO_2 incorporated is a third order polynomial of the form $y = Ax^3 + Bx^2 + Cx + k$ where y represents the microhardness, $\text{Hk}_{50\text{gf}}$ and Vol% of ZrO_2 incorporated in the coating while x is the pH of the electrolyte. A, B, C and k are the deposition constants specific to the composite system being electrodeposited. The constants were calculated from the experimental data by means of a regression program and they are given in Table 1.

Table 1. Constants and the correlation coefficient between Microhardness of the coating and pH of the electrolyte

	A	B	C	k	R^2
Microhardness, Hk	20	-238.57	940	-779.71	0.9073
Vol % of ZrO_2 incorporation	-15.333	153.29	-494.67	531.46	0.9648

The correlation coefficient R^2 has been found to be greater than 0.90 which conveys that the experimental data is in good agreement with the equation. The maximum micro-

hardness (450Hk) and percentage of incorporation is seen for a pH value of 4.0, hence, further studies have been confined to this pH. Xiaozhen et al have reported similar results for 40nm ZrO₂ incorporated in Ni matrix.⁷

The influence of current density on the extent of ZrO₂ incorporation and also on the microhardness is shown in Figure2. It is seen from the figure that the best fitting relation is a second order polynomial of the form $y = ax^2 - bx + c$ with a correlation coefficient greater than 0.95.

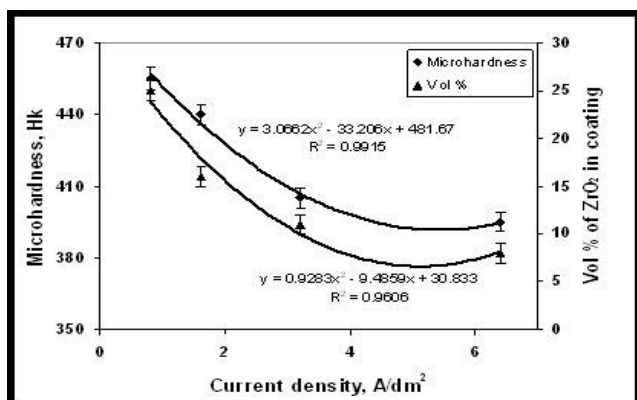


Figure 2. Influence of current density on Microhardness and Vol% of ZrO₂ incorporated in the coating

This shows that the experimental data is in good agreement with the polynomial equation. Here y is the microhardness and Vol % of ZrO₂ incorporated in the coating, x is the current density, Adm^{-2} and a , b and c are the constants whose values are mentioned in Table 2.

Table 2. Constants and the correlation coefficient between Microhardness of the coating and applied current density

	a	b	c	R ²
Microhardness, Hk	3.0662	-33.206	481.67	0.9915
Vol % of ZrO ₂ incorporation	0.9283	-9.4859	30.833	0.9606

A mathematical correlation between current density and ZrO₂ content in the coating has been reported by Benea et al.¹⁸ The maximum microhardness as well as ZrO₂ incorporation is seen for a low current density of 0.8Adm^{-2} hence, the Ni-ZrO₂ and Ni-Co-ZrO₂ nano-composite electroforming was carried out at pH 4.0 and current density of 0.8Adm^{-2} . This observation can be associated with the fact that during electrodeposition at lower current density (0.8Adm^{-2}), the number of collisions between the particles and the cathode surface per unit volume of deposited matrix increases, thus allowing more particles to be incorporated into the coating. Similar observation has been made by Banovic et al for Ni-Al₂O₃ composites.²⁸ The current efficiency was seen to be in the range of 94-98% with increase in current density from 0.8 to 6.4Adm^{-2} .

3.2. Surface Morphology and Structure of Ni-ZrO₂ Composite

The amount of ZrO₂ incorporated in the Ni-ZrO₂ nano-composite electroforms was seen to be about 2wt% by EDX

analysis. Wang et al have reported 2.70wt% of nano ZrO₂ (10-30nm) incorporation in Ni matrix obtained by electrodeposition from a Watt's bath.²¹ Simunkova et al have reported higher (9wt%) incorporation of 200nm size ZrO₂ particles in Ni matrix compared to 40nm size particles (3wt%).⁸ Thus, other researchers have also obtained similar amount of nano ZrO₂ particle incorporation in Ni matrix. The mechanism of ZrO₂ incorporation has been reported by Wang, Benea et al.^{21,18}

The SEM micrograph depicting the surface morphology of the composite electroforms is shown in Figure3. It is seen from Figure3a that agglomerates of nano ZrO₂ particles are distributed on the surface of pyramidal shaped Ni crystallites. A similar morphology of ZrO₂ agglomerates non-uniformly distributed throughout the Ni matrix has been reported by Hou et al.²⁰

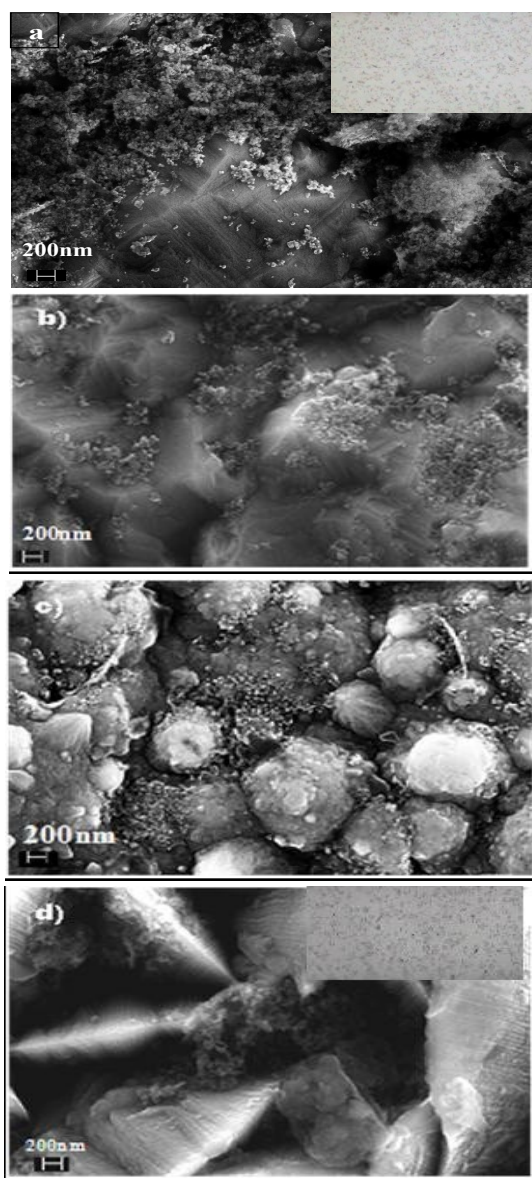


Figure 3. Surface morphology of (a) Ni-ZrO₂ composite coating; Insert shows the cross-sectional optical micrograph (b) Ni-10Co-ZrO₂, (c) Ni-28Co-ZrO₂ and (d) Ni-80-ZrO₂ composite coatings; Insert shows the cross-sectional optical micrograph

However, Wang et al have reported a nodular, smooth morphology for high-speed jet electroplated Ni-ZrO₂ coating.²⁹ The X-ray diffractogram of the Ni-ZrO₂ nano-composites is shown in Figure 4. The coating was found to exhibit a predominant (200) reflection, accompanied with (111). Reddy et al have observed (111) reflection as the predominant peak for pulse electrodeposited Ni-ZrO₂ composite coatings.²³ The difference in the current waveforms employed may be the cause for the difference in the predominant reflections. The crystal structure is seen to be fcc. Reflections corresponding to ZrO₂ are not observed due to the reduced amount (2wt%) of incorporation.

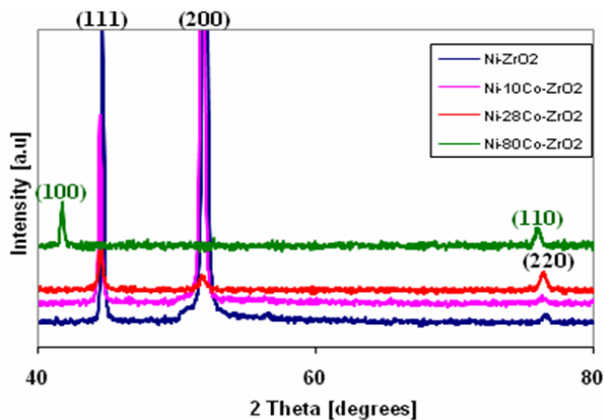


Figure 4. X- ray diffractogram of (a) Ni-ZrO₂, (b) Ni-10Co-ZrO₂, (c) Ni-28Co-ZrO₂ and (d) Ni-80Co-ZrO₂ composite coatings

3.3. Ni-Co-ZrO₂ Co-Deposition

Nano ZrO₂ particles were incorporated in various Ni-Co alloy matrices. The amount of Co incorporated in the composite coatings was in the range of 10-80wt%. The amount of ZrO₂ incorporated in the coatings remained a constant at 2wt% for Co content of 10-28wt%. For a Co content of 80wt% the amount of ZrO₂ particles incorporated increased to 5wt%. Thus, an increase in Co content in the coating has resulted in an increase in ZrO₂ incorporation. This shows that cobalt has better wettability for the particles compared to Ni. Similar observation has been made by the authors for other inert particles like SiC, Si₃N₄.^{27,2} A comparison in the microhardness of Ni-Co alloys and Ni-Co-ZrO₂ composite coatings is depicted in Figure 5.

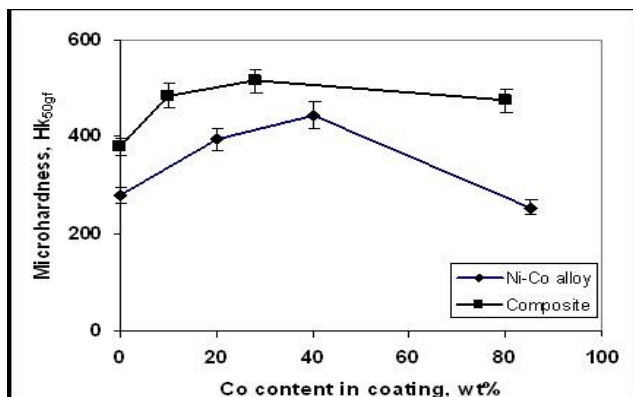


Figure 5. Variation in Microhardness with change in cobalt content in the coating

It is seen from the figure that the microhardness of Ni-Co alloys increases with increase in Co content and attains a maxima followed by a decrease in hardness with increase in Co content. The maximum is observed for a Co content of 40wt%. The decrease in microhardness with increase in Co content is associated with the formation of hcp phase. The incorporation of nano ZrO₂ particles has increased the microhardness of all the Ni-Co alloys. It is also seen that for a constant Co content in the electrolyte in the presence of ZrO₂ particles, a reduction in the Co co-deposition has occurred. This shows that the Co incorporation depends on the nature of the particle co-deposited along with it apart from other deposition conditions. A similar observation has been made by the authors during Si₃N₄ incorporation in Ni-Co matrix.³⁰ This aspect needs to be explored further.

A significant increase in the microhardness of the composites is seen in comparison with that of the plain Ni-Co alloys. The microhardness of the composite increased from 380Hk to a maximum of 515Hk followed by a marginal drop to 475Hk (Figure 5). The maximum is observed for a Co content of 28wt% in the composite, unlike 40wt% in the alloy. An increase in Co content to 80wt% resulted in a marginal reduction to 475Hk. It is seen that ZrO₂ incorporation has significantly improved the microhardness of Co rich Ni-Co alloys. The trend of microhardness reaching a maxima followed by a drop with increase in Co content is similar to that displayed by Ni-Co alloys.³⁰ This behaviour has been associated with the change in the crystal structure from fcc to hcp with increase in Co content.²⁷ The trend in microhardness can also be related to the change in crystallite size. The variation in crystallite size follows the trend of Ni-ZrO₂ (38nm) > Ni-10Co-ZrO₂ (36nm) > Ni-28Co-ZrO₂ (15nm) < Ni-80Co-ZrO₂ (17nm). Thus, it is seen that the high microhardness of Ni-28Co-ZrO₂ composite can be related with its small crystallite size of 15nm which is in accordance with the Hall-Petch relation.

The surface morphology of the Ni-Co-ZrO₂ nano-composites is shown in Figure 3. It is seen from Figs. 3a and 3b that surface morphology of Ni-2ZrO₂ and Ni-10Co-2ZrO₂ composite coatings are similar i.e. the introduction of 10wt% Co has not altered the morphology of Ni matrix. However, in the presence of 28wt% Co in the matrix, a transformation from distinct pyramidal crystallite morphology to irregular nodular is seen in Figure 3c. Irregular pyramidal matrix morphology was seen for Ni-20Co alloy.²⁹ This difference in the matrix morphology is caused by ZrO₂ incorporation. An increase in Co content to 80wt%, the matrix morphology transformed to a ridged structure (Figure 3d). A similar morphology has also been exhibited by Ni-80Co alloy. Thus, it is seen that for higher Co contents and very low Ni contents, the ZrO₂ incorporation has no influence on the matrix morphology. The changes in the surface morphology for higher Co content are due to the change in the crystal structure from fcc to hcp. A similar change has been observed by the authors for Ni-Co alloys and their other composites.^{27,2} The X-ray diffractogram of Ni-Co-ZrO₂ nano-composite coatings is shown in Figure 4. It is seen from the figure that upto 10wt%Co content in the coatings, the predominant

reflection is (200) accompanied with a weak (111) reflection. Similar diffractogram has been exhibited by plain Ni coating.

The Ni-28Co-2ZrO₂ nano-composite exhibited a predominant (111) orientation accompanied with (200) and (220) reflections. The Ni-20Co alloy was seen to exhibit predominant (200) reflection. This change in the reflections may be the cause for the difference in the morphology between the alloy and composite. This change in the preferred orientation from (200) to (111) is also responsible for the higher microhardness of this composite compared to Ni-10Co-2ZrO₂. All the Ni rich composite coatings exhibited fcc crystal structure and as the ZrO₂ incorporation was less, the reflections corresponding to the particles were not seen in the diffractograms. The Co rich Ni-80Co-5ZrO₂ nano-composite exhibited hcp crystal structure with a predominant (100) reflection along with (110). The reflections corresponded to those of hcp Co.

3.4. Influence of Annealing Treatment on Microhardness

The influence of annealing temperatures on the microhardness of Ni-ZrO₂ and Ni-Co-ZrO₂ nano-composites is shown in Figure 6. It is seen from the figure that the trend followed by the Ni and Ni-Co composites is similar to that of plain Ni and Ni-Co alloy coatings. The microhardness of Ni-2ZrO₂ nano-composite is stable upto 400°C with no significant change in the values. The variation in microhardness of Ni-ZrO₂ coatings with annealing temperature has also been studied by Reddy et al.²³ They have observed an initial rise in the values upto 200°C followed by a drastic reduction at 300°C and subsequently a slow but continuous decrease at 600°C. The cause for the difference in behaviour between Reddy's and present study is, the composite studied by former is pulsed co-deposited and the ZrO₂ particles have tetragonal crystal structure²³ while, the deposition in the present study is direct current deposition and the particles have monoclinic structure. The microhardness of Ni-10Co-2ZrO₂ composites is higher than that of Ni-2ZrO₂ composite.

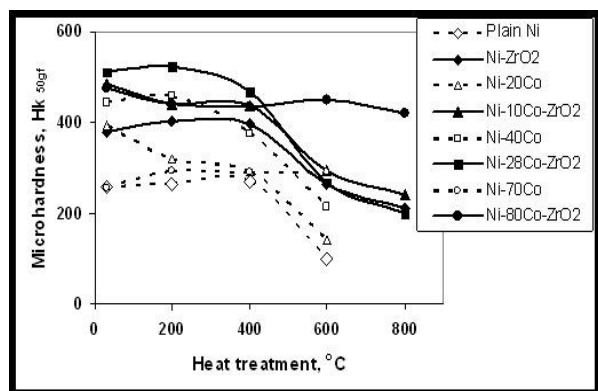


Figure 6. Influence of temperature on the microhardness of Ni-ZrO₂ and Ni-Co-ZrO₂ composite coatings

A 9% reduction in microhardness is seen at a temperature of 400°C compared to ambient temperature microhardness. This trend has been observed for all the Ni-Co-ZrO₂ nano-

composites, irrespective of the Co content in the matrix. At temperatures of 600°C, Ni-ZrO₂ coating exhibited a reduction in microhardness of about 30% (relative to ambient condition). While, Ni-Co-ZrO₂ nano-composites exhibited a reduction of 37% and 47% for a Co content of 10wt% and 28wt% in the matrix respectively. Only a 5% reduction in microhardness is observed at 600°C for Ni-80Co-5ZrO₂ composite coating. This shows that this nano-composite possesses better stability in terms of microhardness compared to the other Ni-Co-ZrO₂ and Ni-ZrO₂ composites. A further increase in the annealing temperature has resulted in above 50% decrease in the microhardness for Ni-2ZrO₂, Ni-10Co-2ZrO₂ and Ni-28Co-2ZrO₂ nano-composites. This confirms that the microhardness of Ni rich ZrO₂ composites is less stable at temperatures beyond 600°C. The Ni-80Co-5ZrO₂ nano-composite displays only an 11% reduction in the values even at temperatures of 800°C thereby showing its better stability compared to all the other three coatings studied.

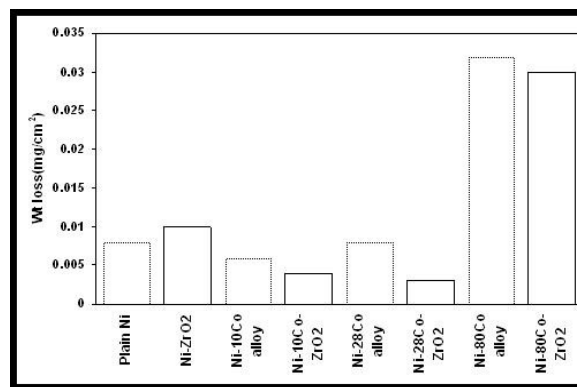


Figure 7. Comparative weight loss of Ni-ZrO₂ and Ni-Co-ZrO₂ composites after immersion in 3.5%NaCl for 168hours

3.5. Corrosion Behaviour

3.5.1. Immersion Corrosion

The corrosion rate expressed in terms of weight loss on immersion in 3.5%NaCl is shown in Figure 7. It is seen from the figure that the weight loss of coating on immersion in NaCl is marginally less for the ZrO₂ incorporated Ni-Co composites compared to Ni-Co alloy coatings. In other words, the corrosion resistance of the composite coatings is better, although to a smaller extent, compared to the plain coatings. It is also seen that the weight loss of Ni-28Co-ZrO₂ composite is less compared to Ni-ZrO₂ and other Ni-Co-ZrO₂ composite coatings. Thus, it can be concluded that the corrosion resistance of Ni-Co alloy and the composite possessing Co content close to 25 ± 5wt% is better compared to plain Ni, its composite and other Ni-Co alloys, their composites. Similar observation for the Ni-Co alloys has been observed by the authors in earlier studies using Potentiodynamic polarization and Impedance analysis.³⁰ Another conclusion that can be drawn from the figure is that an increase in weight loss is seen with increase in Co content in the coatings. Thus, revealing that Co rich Ni-Co

coatings have poor corrosion resistance.

The composite coatings exposed to the corrosive medium of 3.5% NaCl were subjected to FESEM analysis to study the surface morphology, and EDX analysis to identify the compositional changes. The surface morphology of the coatings after immersion in the corrosive medium are displayed in Figure 8 and the elemental composition is shown in Table 3. Ni-ZrO₂ coating after immersion in the corrosive medium shows the presence of deep depressions (Figure 8a). The EDX analysis revealed that the zirconia content within the depression is less compared to that in the matrix (Table 3).

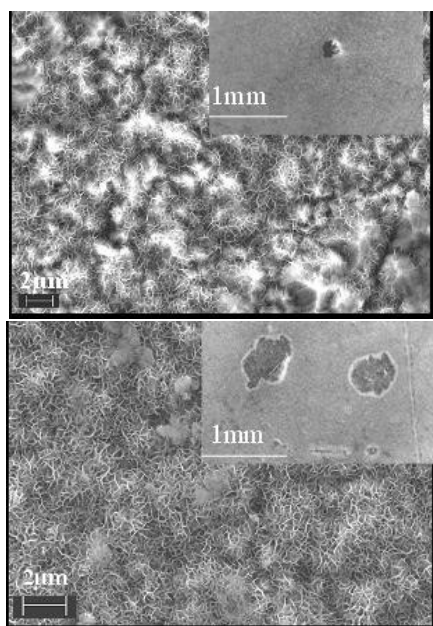


Figure 8. Surface morphology of corroded surface of (a) Ni-ZrO₂, (b) Ni-10Co-ZrO₂ composite coatings; Inset shows the image at low magnification

This confirms the occurrence of dislodgement of ZrO₂ particles. A change in the matrix morphology is also seen.

Table 3. Elemental composition analysis of Ni-ZrO₂ and Ni-Co-ZrO₂ composite coatings prior to and after immersion in corrosive medium, 3.5% NaCl

	Ni-ZrO ₂	Ni-10Co-ZrO ₂	Ni-28Co-ZrO ₂	Ni-80Co-ZrO ₂
Ni wt% Before	Bal	Bal	Bal	Bal
After	Bal	Bal	Bal	Bal
Co wt% Before	-	10	28	80
After	-	9m, 7p	30m, 29p	64
Zr wt% Before	2	2	2	5
After	3m, 1p	4m, 2p	1.45m, 1.69p	5.6
Cl wt% Before	-	-	-	-
After	0.41m, 15.0p	0.8m, 14.0p	0.3m, 5.0p	1.0
O wt% Before	-	-	-	-
After	13m, 29p	23m, 28p	12m, 15p	21

p – depression, m-matrix, Bal-Balance

Depressions are seen in the case of Ni-10Co-ZrO₂ composite coating also as shown in Figure 8b. It is seen from EDX analysis that the zirconia and cobalt content within the depression are less compared to the matrix. This also confirms the removal of the particles. Also, the chlorine and oxygen contents are higher within the depression (Figure 8c) compared to the matrix. The surface morphology of Ni-28Co-ZrO₂ composite coating is shown in Figure 8d. It is seen from the figure that very shallow depressions are formed along with a nodular matrix. No appreciable change in the surface morphology is seen after immersion. The EDX analysis illustrates no appreciable change in the zirconia content. Also, the change in the concentration of chlorine and oxygen contents are seen to be less in the shallow depressions compared to those observed in Ni-10Co-ZrO₂ and Ni-ZrO₂ coatings. This shows that the corrosion resistance of Ni-28Co-ZrO₂ composite is better compared to the other coatings. This is in correlation with the low weight loss of this coating compared to the other coatings studied. The surface morphology of Ni-80Co-ZrO₂ composite coating is shown in Figure 8e. No depression is seen but the surface appears to be loosely packed branched thin filaments, causing the penetration of the corrosion-active species within the coating. The EDX analysis revealed a drastic reduction in Co content from 80wt% to 64wt% thus, confirming the dissolution of the matrix (Table 3).

Thus, the increased corrosion rate of the Co rich Ni-Co-ZrO₂ composite can be attributed to the dissolution of the matrix.

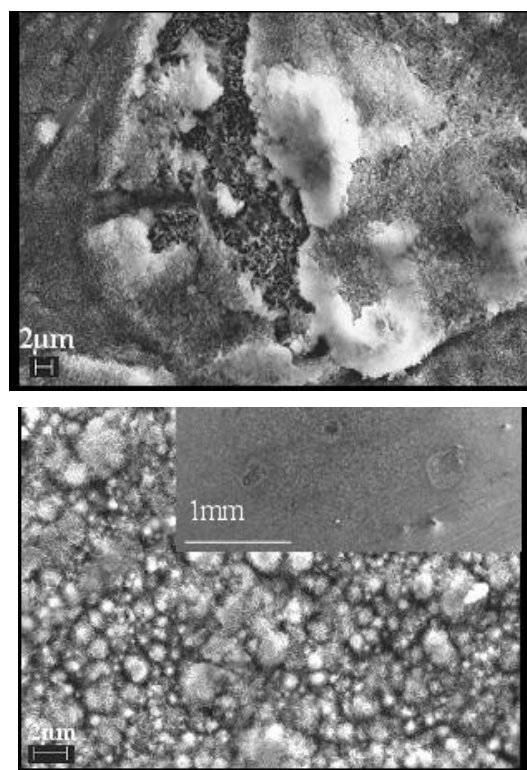


Figure 8. Surface morphology of corroded surface of (a) Ni-ZrO₂, (b) Ni-10Co-ZrO₂, (c) higher magnification image of Ni-10Co ZrO₂ composite, (d) Ni-28Co-ZrO₂ and (e) Ni-80-ZrO₂ composite coatings; Inset shows the image at low magnification

3.4.2. Polarization Studies

The corrosion behaviour of the coatings was analyzed by Polarization studies and the polarization curves are displayed in Figure 9.

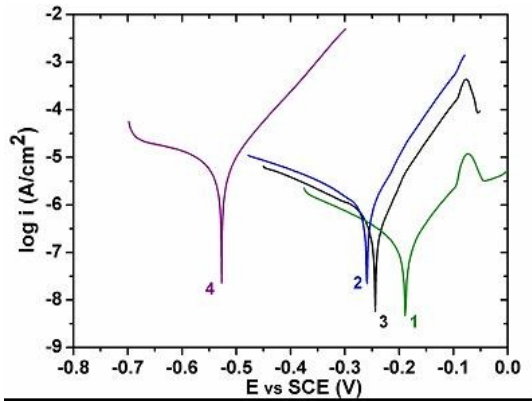


Figure 9. Polarization curves of Ni-ZrO₂ (1), Ni-10Co-ZrO₂ (2), Ni-28Co-ZrO₂ (3) and Ni-80Co-ZrO₂ (4) composites

The electrochemical parameters – corrosion current density i_{corr} and corrosion potential E_{corr} obtained from Potentiodynamic polarization studies are listed in Table 4.

Table 4. Corrosion parameters obtained from Polarization studies

Coating	E_{corr} , V	I_{corr} , $\mu\text{A}/\text{cm}^2$
Ni-ZrO ₂	-0.189	0.170
Ni-10Co-ZrO ₂	-0.259	0.853
Ni-28Co-ZrO ₂	-0.244	0.574
Ni-80Co-ZrO ₂	-0.527	7.325

The corrosion current i_{corr} for plain Ni is found to be $1.060\mu\text{A}/\text{cm}^2$. The incorporation of ZrO₂ in Ni matrix reduced the corrosion current to $0.170\mu\text{A}/\text{cm}^2$. This indicates that the addition of ZrO₂ in Ni matrix has improved its corrosion resistance. The reinforcement of ZrO₂ in Ni-Co matrices follows the trend Ni-28Co-ZrO₂ ($0.574\mu\text{A}/\text{cm}^2$) < Ni-10Co-ZrO₂ ($0.853\mu\text{A}/\text{cm}^2$) < Ni-80Co-ZrO₂ ($7.325\mu\text{A}/\text{cm}^2$). It is seen that the least corrosion current value i.e in other words better corrosion resistance is displayed by Ni-28Co-ZrO₂ coating compared to the other Ni-Co-ZrO₂ composites. The corrosion potential E_{corr} of plain Ni is found to be -0.326V, the incorporation of ZrO₂ in Ni matrix resulted in a positive shift in potential to -0.189V. This indicates that the addition of ZrO₂ in Ni matrix has improved the corrosion resistance. It is also seen from the table that no significant change in the E_{corr} values is seen between Ni-10Co-ZrO₂ (-0.259V) and Ni-28Co-ZrO₂ (-0.244V) however, the values are less positive compared to Ni-ZrO₂ coating. This conveys that the corrosion resistance of Ni-ZrO₂ composite is better compared to Ni-Co-ZrO₂ composites. An increase in Co content in the matrix to 80wt% resulted in a significant shift to more negative value (-0.527V) indicating its poor corrosion behaviour compared to all the coatings studied. Thus, it is understood that addition of cobalt beyond 28wt% impairs the beneficial corrosion

effect of Ni.

3.4.3. Electrochemical Impedance Studies

The impedance plots of Ni-ZrO₂ and Ni-Co-ZrO₂ composites with various cobalt contents are shown in Figures 10 and 11. Figure 10 represents the Nyquist plot. The interception of Z' in the Nyquist plot at higher frequencies is ascribed as electrolytic bulk resistance R_s and at lower frequencies the interception is ascribed as the charge transfer resistance R_{ct} .

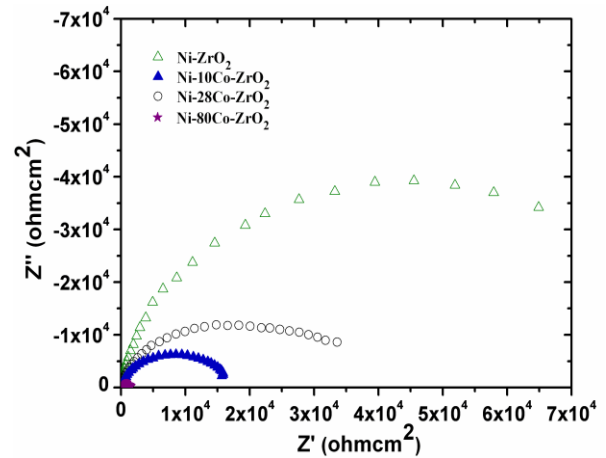


Figure 10. Nyquist plots of Ni-ZrO₂, Ni-10Co-ZrO₂, Ni-28Co-ZrO₂ and Ni-80Co-ZrO₂ composites

The Nyquist plot shows single semicircle for Ni-ZrO₂ and Ni-Co-ZrO₂ composite coatings and this can be associated with single time constant i.e. the charge transfer process in the coating/electrolyte interface. Bode plot of frequency vs phase angle (Fig.11) displayed a single, broad peak indicating the large capacitive behaviour of the coatings. The single peak corresponded to the coating electrolyte (3.5% NaCl) interface.

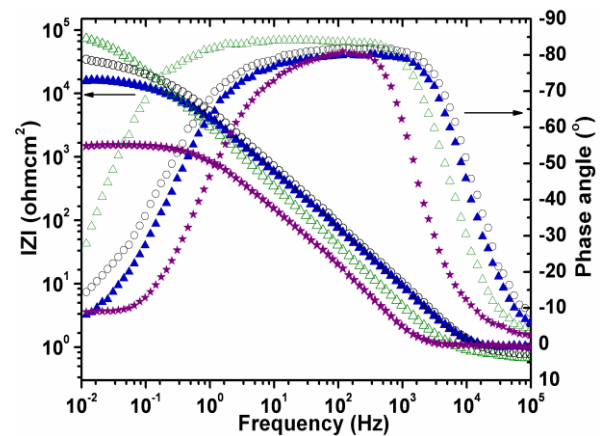


Figure 11. Bode Plots of Ni-ZrO₂, Ni-10Co-ZrO₂, Ni-28Co-ZrO₂ and Ni-80Co-ZrO₂ composites

This behaviour can be modeled as a parallel combination of a double layer capacitance C_{dl} and a charge transfer resistance R_{ct} both of which are in series with the solution resistance R_s between the working electrode WE and the tip of the Luggin capillary. The simple Randles circuit described as R(QR) was used for fitting the plots obtained for the

coatings studied and the fitted values are displayed in Table 5. The double layer capacitance provides information about the polarity and the amount of charge at the coating electrolyte interface.

Table 5. Electrochemical parameters obtained from Impedance studies of Ni-ZrO₂ and Ni-Co-ZrO₂ composites

Coating	Rs, Ω cm ²	Q _{dl} , μS s ⁿ cm ⁻²	n	R _{ct} , kΩ cm ²
Ni-ZrO ₂	0.90	31.6	0.94	83.87
Ni-10Co-ZrO ₂	0.91	42.8	0.90	15.91
Ni-28Co-ZrO ₂	0.89	34.6	0.93	32.90
Ni-80Co-ZrO ₂	1.10	79.7	0.89	1.534

The R_{ct} values obtained increased in the order: Ni-ZrO₂, Ni-28Co-ZrO₂, Ni-10Co-ZrO₂ and Ni-80Co-ZrO₂. The R_{ct} value being the highest for Ni-ZrO₂ coating indicates that the active area available for corrosive attack is less or alternatively the corrosion resistance is better compared to the others. The capacitance C is represented by a general diffusion related element Q which is defined as a constant phase element. This accounts for the deviation from the ideal dielectric behaviour and is related to surface inhomogeneity. This element is mathematically written in the admittance form as $Y^*(\omega) = Y_0 (j\omega)^n$ where, Y₀ is an adjustable parameter used in the non-linear least square fitting and n is an adjustable parameter in the range of 0.5 to 1. The value of n is obtained from the slope of frequency vs $|Z|$ plot (Fig. 11). The phase angle θ can vary between 90° (for a perfect capacitor n=1) to 0° (for a perfect resistor n=0). It is understood from Table 5 that Q_{dl} value is very low for Ni-ZrO₂ compared to Ni-Co-ZrO₂. Among the Ni-Co-ZrO₂ composites, Ni-28Co-ZrO₂ composites display lower values and close to Ni-ZrO₂ compared to Ni-10Co-ZrO₂ and Ni-80Co-ZrO₂ composites. This indicates that addition of around 28wt% of Co improved the surface morphology of the coating and decreased the surface defects and further increase or decrease in cobalt contents resulted in a reverse effect. Further, the n_{dl} values are 0.93 and 0.94 for Ni-28Co-ZrO₂ and Ni-ZrO₂ composites respectively indicating low capacitive behaviour of these coatings. Whereas, the values are 0.89, 0.90 for Ni-80Co-ZrO₂ and Ni-10Co-ZrO₂ coatings respectively indicating further lower capacitive behaviour of the coatings. Bode plot Fig. 11 shows that θ for Ni-ZrO₂ and Ni-28Co-ZrO₂ coatings are almost 85° whereas it is 80° for Ni-10Co-ZrO₂ and Ni-80Co-ZrO₂ coatings. This also shows that the capacitive behaviour of the former coatings is better compared to the latter.

A difference in the corrosion behaviour is seen between the immersion and polarization studies. Ni-28Co-ZrO₂ composite is seen to display better immersion corrosion resistance in terms of weight loss while, the Electrochemical studies showed that Ni-ZrO₂ composite displays better corrosion resistance.

3.6. Wear Behaviour

The comparative wear volume loss for plain Ni, Ni-Co

alloys and Ni/Ni-Co-ZrO₂ composite coatings is listed in Table 6. It is seen from the table that the wear volume loss for the composite coatings is remarkably less compared to that of plain Ni and Ni-Co alloy coatings.

Table 6. Comparative wear volume loss observed in Ni-ZrO₂ and Ni-Co-ZrO₂ composites

Coating	Wear volume loss X10 ⁻⁴ mm ³ /m
Plain Ni	4.35
Ni-28Co	0.88
Ni-70Co	2.54
Ni-ZrO ₂	1.73
Ni-10Co-ZrO ₂	0.0083
Ni-28Co-ZrO ₂	0.0119
Ni-80Co-ZrO ₂	0.764

The Ni-20Co alloy is seen to display the least material volume loss i.e. better wear resistance. It is also seen that the addition of Co to Ni improves the wear resistance irrespective of the Co content added. The volume loss for the Ni-Co-ZrO₂ composites follows the order: Ni-10Co-ZrO₂, Ni-28Co-ZrO₂ < Ni-80Co-ZrO₂ < Ni-ZrO₂. This may be correlated to their microhardness values. Thus, the wear behaviour is in accordance with the Archard's law wherein the wear resistance is proportional to the microhardness. The material volume loss is seen to increase significantly for Ni-80Co-5ZrO₂ composite similar to that of Ni-80Co alloy. However, the increase is less compared to Ni-ZrO₂ composite. This shows that the addition of Co to Ni improves its wear resistance even in the presence of ZrO₂ particles.

4. Conclusions

The effect of nano ZrO₂ incorporation in Ni and Ni-Co matrix was studied by developing Ni-ZrO₂ and Ni-Co-ZrO₂ composites through electrodeposition method under optimized conditions with respect of microhardness. The FE-SEM studies showed that the surface morphology of Ni-ZrO₂ composites comprised of polyhedral crystallites along with agglomerated ZrO₂ particles. However, the surface morphology of Ni-Co-ZrO₂ composites depended on the Co content. A change in morphology from polyhedral-nodular-ridged was observed with increase in Co content from 10wt% - 80wt%. A change in crystal structure from fcc to hcp was seen for a similar change in Co content. It was observed from the thermal stability studies that the stability in terms of microhardness was higher for Co rich Ni-80Co-5ZrO₂ composite coating upto temperatures of 800°C compared to Ni-ZrO₂ and other Ni rich Ni-Co-ZrO₂ composite coatings. The immersion corrosion studies revealed that the corrosion occurred by localized pitting in the case of Ni rich Ni-Co/Ni composites and that the corrosion rate was the least in Ni-28Co-ZrO₂ composite coating. Ni-80Co-5ZrO₂ composite displayed uniform and higher corrosion rate compared to Ni rich composites. However, the polarization and electrochemical studies showed that the corrosion behaviour of Ni-ZrO₂ composite was better than that of Ni-Co composites. However, the behaviour of Ni-28Co-ZrO₂ coating is very

close to that of Ni-ZrO₂ coating. It was seen from the wear studies that Ni-10Co-2ZrO₂, Ni-28Co-2ZrO₂ composites displayed better wear resistance. Thus, Ni-28Co-2ZrO₂ composite appears to be optimum in terms of corrosion and wear resistance. Depending on the functional requirement, Ni-Co-ZrO₂ composite coatings can be tailor made to meet different needs.

ACKNOWLEDGEMENTS

The authors would like to thank the Director, NAL for permission to carry out this study. A special word of thanks to Mr.Siju, Ms.Latha and Mr.Muniprakash for their assistance in performing the FESEM, microhardness and wear analysis. Ms.Kavitha is also acknowledged for her assistance in performing the experiments.

REFERENCES

- [1] Robertson, A, Erb, U, Palumbo, G, 1999, "Practical applications for electrodeposited nanocrystalline materials." *Nanostruct. Mater.*, 12, 1035-1040
- [2] Wang, W, Qian, SQ, Zhou XY, 2010, "Microstructure and Oxidation-resistant of ZrO₂/Ni coatings applied by high-speed jet electroplating." *J. Mater. Sci.*, 45, 1617-1621
- [3] Gul H, Kihc F, Aslan S, Alp A, Akbulut H, 2009, "Characteristics of electro-co-deposited Ni-Al₂O₃ nano- particle reinforced metal matrix composite (MMC) coatings." *Wear*, 267, 976-990
- [4] Wang S-C, Wei W-C. J,2003, "Kinetics of electroplating process of nano-sized ceramic particle/Ni composite." *Mater. Chem. Phys.*, 78, 574-580
- [5] Carac G, Benea L, Iticescu C, Lampke T, Steinhauser S, Wielage B, 2004, "Codeposition of cerium oxide with nickel and cobalt : Correlation between microstructure and microhardness." *Surf. Eng.*, 20, 353-359
- [6] Liu Y, Ren L, Yu S, Han Z, 2008, "Influence of current density on nano-Al₂O₃/Ni+Co bionic gradient composite coatings by electrodeposition." *J. Univ. Sci. Technol.*, 15, 633-637.
- [7] Xiaozhen L, Xin L, Aibing Y, Weijue H, 2009, "Preparation and Tribological performance of electrodeposited Ni-TiB₂-Dy₂O₃ composite coatings." *J. Rare Earth*, 27, 480-485
- [8] Simunkova H, Garcia P.P, Wosik J, Angerer P, Kronberger H, Nauer G. E, 2009, "The fundamentals of nano- and submicro-scaled ceramic particle incorporation into electrodeposited Ni layers : Zeta potential measurements." *Surf. Coat.Technol.*, 203, 1806-1814
- [9] Balathandan S, Annamalai V.E, Seshadri S.K, 1992, " Electrocomposite coating of partially stabilized zirconia dispersed in a nickel matrix." *J. Mater. Sci. Lett.*, 11, 449-451
- [10] Qu N.S, Zhu D, Chan K.C, 2006, " Fabrication of Ni-CeO₂ nanocomposite by Electrodeposition." *Scripta Mater.*, 54, 1421-1425
- [11] Gomez E, Pane S, Valles E, 2005, " Electrodeposition of Co-Ni and Co-Ni-Cu systems in sulphate-citrate medium." *Electrochim. Acta*, 51, 146-153
- [12] Wang L, Gao Y, Xue Q, Liu H, Xu T, 2005, "Microstructure and Tribological properties of electrodeposited Ni-Co alloy deposits." *Appl. Surf. Sci.*, 242, 326-332
- [13] Wang W, Guo H.T, Gao J.P, Dong X.H, Qin Q.X, 2000, "XPS, UPS and ESR studies on the interfacial interaction in Ni-ZrO₂ composite plating." *J. Mater. Sci.*, 35, 1495-1499
- [14] Setare E, Raeissi K, Golozar M.A, Fathi M.H, 2009, "The structure and corrosion barrier performance of nanocrystalline zirconia electrodeposited coating." *Corros. Sci.*, 51, 1802-1808
- [15] Valov, Stoychev D, Marinova Ts, 2002, " Study of the kinetics of process during electrochemical deposition of zirconia from nonaqueous electrolytes." *Electrochim. Acta*, 47, 4419-4431
- [16] Stoychev D, Ikononov J, Robinson K, Stefanov P, Stoycheva M, Marinova Ts, 2000, "Surf. Interface Anal.", 30, 69-73
- [17] Rajiv E.P, Annamalai V.E, Seshadri S.K, 1992, "Transformation - toughened cobal - partially stabilized zirconia electrocomposite coating," *J. Mater. Sci.*, 11, 466-468
- [18] Benea L, Lakatos-Varsanyi M, Maurin G, 'The Annals of Dunarea De Jos' University of Galati Fascicle IX Metallurgy and Materials Science, ISSN 1453-083X NR.II- 2003,10-17
- [19] Zhang K.F, Ding S, Wang G.F, 2008, "Different superplastic deformation behaviour of nanocrystalline Ni and ZrO₂/Ni nanocomposite." *Mater. Lett.*, 62, 719-722
- [20] Hou F, Wang W, Guo H, 2006, "Effect of the dispersibility of ZrO₂ nanoparticles in Ni-ZrO₂ electroplated nanocomposite coatings on the mechanical properties of nanocomposite coatings." *Appl. Surf. Sci.*, 252, 3812-3817
- [21] Wang, Hou F-Y, Wang H , Guo H-T, 2005, "Fabrication and characterization of Ni-ZrO₂ composite nano-coatings by pulse electrodeposition." *Scripta Mater.*, 53, 613-618
- [22] Moller A, Hahn H, 1999, "Synthesis and Characterization of Nanocrystalline Ni/ZrO₂ composite coating." *NanoStruct. Mater.*, 12, 259-262
- [23] Reddy B.S.B, Das K, Datta A.K, Das S, 2008, "Pulsed co-electrodeposition and characterization of Ni-based nanocomposites reinforced with combustion-synthesized, undoped, tetragonal-ZrO₂ particulates." *Nanotech.*, 19, 15603-115613
- [24] Ramesh Babu G.N.K, Jayakrishnan S, 2006, "Oxidation characteristics of electrodeposited nickel-zirconia composites at high temperatures." *Mat. Chem. Phys.*, 96, 321-325
- [25] Zhang J, Wang D.-Y, Sun Z.-F, Zhao W.-L, Guo X.-Y, "Wuhan Ligong Daxue Xuebao/J.Wuhan Univ. Tech.", 2008, 30: 21
- [26] H Klung, L Alexander, "X-ray Diffraction Procedures for Polycrystalline and Amorphous materials", 618 John Wiley, New York (1974)

- [27] Srivastava M, William Grips V.K, Rajam K.S, 2007, "Electrochemical deposition and Tribological behaviour of Ni and Ni-Co metal matrix composites with SiC nano-particles." *Appl. Surf. Sci.*, 253, 3814-3824
- [28] S.W Banovic, B.F Levin, J.N DuPont, A.R Marder, 'Progress Report prepared for U S Department of Energy under Grant No. DE-FG22-95PC95211', Project Period: 7/14/95-12/31/97
- [29] Srivastava M, William Grips V.K, Rajam K.S, 2009, "Influence of Co on Si₃N₄ incorporation in electrodeposited Ni." *J. Alloy Compd.*, 469, 362-365
- [30] Srivastava M, EzhilSelvi V, William Grips V.K, Rajam K.S, 2006, "Corrosion resistance and microstructure of electrodeposited nickel-cobalt alloy coatings." *Surf. Coat. Tech.*, 201, 3051-3060